Inorg. Chem. **2008**, *47*, 705–712

Synthesis, Structure, and Infrared Spectroscopy of the First Np^{5+} Neptunyl Silicates, $Li_6(NpO_2)_4(H_2Si_2O_7)(HSiO_4)_2(H_2O)_4$ and $K_3(NpO_2)_3(Si_2O_7)$

T. Z. Forbes and P. C. Burns*

Department of Civil Engineering and Geological Sciences, University of Notre Dame, 156 Fitzpatrick Hall of Engineering, Notre Dame, Indiana 46556

Received July 5, 2007

Two Np^{5+} silicates, $Li_6(NpO_2)_4(H_2Si_2O_7)(HSiO_4)_2(H_2O)_4$ (*LiNpSi1*) and $K_3(NpO_2)_3(SiO_3OH)_2$ (*KNpSi1*), were synthesized by hydrothermal methods. The crystal structures were determined using direct methods and refined on the basis of F^2 for all unique data collected with Mo Kα radation and an APEX II CCD detector. *LiNpSi1* crystallizes in orthorhombic space group *Pnma* with a =13.189(6) Å, b = 7.917(3) Å, c = 10.708(5) Å, V = 1118.1(8) Å^3, and Z = 2. *KNpSi1* is hexagonal, $P\bar{6}2m$, a = 9.734(1) Å, c = 3.8817(7) Å, V = 318.50(8) Å^3, and Z = 1. *LiNpSi1* contains chains of edge-sharing neptunyl pentagonal bipyramids linked into two-dimensional sheets through direct linkages between the neptunyl polyhedra and the vertex sharing of the silicate tetrahedra. The structure contains both sorosilicate and nesosilicate units, resulting in a new complex neptunyl silicate sheet. *KNpSi1* contains edge-sharing neptunyl square bipyramids linked into a framework structure through the sharing of vertices with the silicate tetrahedra. The neptunyl silicate framework contains channels approximately 6.0 Å in diameter. These structures exhibit significant departures from other reported Np^{5+} and U^{6+} compounds and represent the first reported Np^{5+} silicate structures.

Introduction

Silicates are structurally highly complex.[1] Almost all actinyl silicate structures known contain the uranyl ion. These include some of the most important of the uranyl minerals.[2] The structures of uranyl silicate compounds were reviewed by Burns.[3] The uranophane group consists of minerals based upon sheets of uranyl pentagonal bipyramids and silicate tetrahedra, with various lower-valence cations located in the interlayer regions.[4−10] The minerals haiweeite ($Ca[(UO_2)_2Si_5O_{12}(OH)_2](H_2O)_3$)[11] and weeksite ($K_{1.26}Ba_{0.25}Ca_{0.12}[(UO_2)_2(Si_5O_{13})]H_2O$)[12] contain a sheet that is related to that of the uranophane group but that incorporates more silicate tetrahedra by including a chain of tetrahedra. Soddyite $(UO_2)_2(SiO_4)(H_2O)_2$ possesses a framework structure that is composed of chains of edge-sharing uranyl pentagonal bipyramids that are cross-linked by sharing equatorial edges with silicate tetrahedra.[13] Synthetic framework uranyl silicates, such as $KNa_3(UO_2)_2(Si_4O_{10})_2(H_2O)_2$ [14] and $Na_4(UO_2)_2(Si_4O_{10})_2(H_2O)_4$,[15] contain sheets of polymerized silicate tetrahedra that are cross-linked into a framework by the sharing of vertices with uranyl square bipyramids. The compound $RbNa(UO_2)(Si_2O_6)(H_2O)$[16] contains rings of four silicate tetrahedra that are linked into a framework by sharing vertices with uranyl square bipyramids. Thus, uranyl silicates have been shown

* To whom correspondence should be addressed. E-mail: pburns@nd.edu.

(1) Liebau, F. *Structural Chemistry of Silicates: Structure, Bonding, and Classification*; Springer-Verlag: New York, 1985; p 347.
(2) Finch, R.; Murakami, T. Systematics and paragenesis of uranium minerals. In *Uranium: Mineralogy, Geochemistry, and the Environment*; Burns, P. C., Finch, R., Eds.; Mineralogical Society of America: Washington, DC, 1999; Vol. 38, pp 91−180.
(3) Burns, P. C. *Can. Mineral.* **2005**, *43*, 1839.
(4) Ginderow, D. *Acta Crystallogr., Sect. C: Cryst. Struct. Commun.* **1988**, *44*, 421.
(5) Burns, P. C. *Can. Mineral.* **1998**, *36*, 1069.
(6) Burns, P. C. *J. Nucl. Mater.* **1999**, *265*, 218.
(7) Rosenzweig, A.; Ryan, R. R. *Cryst. Struct. Commun.* **1977**, *6*, 617.
(8) Ryan, R. R.; Rosenzweig, A. *Cryst. Struct. Commun.* **1977**, *6*, 611.
(9) Kubatko, K.-A.; Burns, P. C. *Am. Mineral.* **2006**, *91*, 333.
(10) Viswanathan, K.; Harneit, O. *Am. Mineral.* **1986**, *71*, 1489.
(11) Burns, P. C. *Can. Mineral.* **2001**, *39*, 1153.
(12) Jackson, J. M.; Burns, P. C. *Can. Mineral.* **2001**, *39*, 187.
(13) Demartin, F.; Gramaccioli, C. M.; Pilati, T. *Acta Crystallogr., Sect. C: Cryst. Struct. Commun.* **1992**, *48*, 1.
(14) Burns, P. C.; Olson, R. A.; Finch, R. J.; Hanchar, J. M.; Thibault, Y. *J. Nucl. Mater.* **2000**, *278*, 290.
(15) Li, Y.; Burns, P. C. *J. Nucl. Mater.* **2001**, *299*, 219.
(16) Wang, X.; Huang, J.; Liu, L.; Jacobson, A. J. *J. Mater. Chem.* **2002**, *12*, 406.

10.1021/ic701335j CCC: $40.75
Published on Web 12/18/2007

Table 1. Selected Crystallographic Parameters for *LiNpSi1* and *KNpSi1*

	LiNpSi1	*KNpSi1*
formula	$Li_6(NpO_2)_4(H_2Si_2O_7)(HSiO_4)_2(H_2O)_4$	$K_3(NpO_2)_3(Si_2O_7)$
fw	1546.07	1092.48
temp (K)	293(2)	293(2)
cryst syst	*P*nma	$P\bar{6}2m$
a (Å)	13.189(6)	9.734(1)
b (Å)	7.917(3)	
c (Å)	10.708(5)	3.8817(7)
vol (Å^3)	1118.1(8)	318.50(8)
Z	2	1
D_{calcd} (g/cm^3)	4.592	5.780
μ (mm^{-1})	18.77	25.534
F(000)	1348	476
cryst size (mm^3)	0.11 × 0.08 × 0.05	0.21 × 0.01 × 0.01
θ range	2.45−25.00	2.42−34.60
data collected	$-15 < h < 15$, $-9 < k < 9$, $-12 < l < 12$	$15 < h < 15$, $-15 < k < 15$, $-6 < l < 6$
reflns collected/unique reflns	10516/1065	6548/544
refinement method	full-matrix least-squares of F^2	full-matrix least-squares of F^2
data/restraints/params	1065/0/79	544/0/20
GOF on F^2	1.062	1.081
final *R* indices [$I > 2\sigma(I)$]	$R_1 = 0.0455$	$R_1 = 0.0339$, w$R_2 = 0.0564$
R indices (all data)	$R_1 = 0.0806$, w$R_2 = 0.1364$	$R_1 = 0.0363$, w$R_2 = 0.0568$
largest diff. peak and hole (Å^{-3})	3.66 and −2.16	1.52 and −2.44

to be structurally diverse and relatively complex. Synthesis and powder diffraction indicate that the Np^{6+} compounds $K(NpO_2)(SiO_3OH)(H_2O)$[17] and $(NpO_2)_2(SiO_4)(H_2O)_4$ [18] are isostructural with the uranyl silicate minerals boltwoodite (uranophane group) and soddyite, respectively.

An understanding of the solution and crystal chemistry of neptunium is important for the safe disposal of nuclear waste and the remediation of contaminated sites. In contrast to uranium, the most stable oxidation state for neptunium under oxidizing environmental conditions is pentavalent. The crystal chemistry of U^{6+} and Np^{5+} appears to be rather similar to the casual observer, as they both form nearly linear dioxo cations $(UO_2)^{2+}$ and $(NpO_2)^+$, respectively.[19] Each of these actinyl ions also almost invariably occurs in crystal structures coordinated by four, five, or six ligands, giving square, pentagonal, and hexagonal bipyramids. Studies have investigated incorporation of Np^{5+} by substitution for U^{6+} in uranyl phases that form as alteration products of nuclear waste.[20−22] Despite the deceptively similar geometries of uranyl and neptunyl polyhedra, recent studies have revealed that the structural topologies of neptunyl compounds are usually radically different from chemically similar uranyl compounds. The strength of the bonds within the neptunyl ion are somewhat weaker than those in the uranyl ion, and this results in the propensity of cation−cation interactions in the former.[23−31] In a cation−cation interaction, the O atom of one actinyl ion coordinates a second actinyl ion as an equatorial ligand within its bipyramidal polyhedron.[32] The topologies of structures of neptunium compounds that exclude cation−cation interactions are often different from chemically related uranyl compounds.

Here, we report the first Np^{5+} neptunyl silicate structures for two synthetic compounds, $Li_6(NpO_2)_4(H_2Si_2O_7)(HSiO_4)_2(H_2O)_4$ (designated *LiNpSi1*) and $K_3(NpO_2)_3(Si_2O_7)$ (*KNpSi1*). Both present structural topologies that are unprecedented in actinide chemistry.

Experimental Procedures

Crystal Synthesis. $(NpO_2)^+$ was recovered from earlier experiments, dissolved in 1 M $HClO_4$, and purified using a cation exchange column containing Dowex-50-X8 resin. The experimental protocol required precipitation of $(NpO_2)^+$ and redissolution in 1 M HCl. A UV spectrum was collected for the resulting solution to ensure that it contained only pentavalent neptunium. ***Caution!*** *237-Np represents a serious health risk due to the emissions of* α*- and* γ*-radiation. These studies require appropriate equipment and personnel for handling radioactive materials.* Single crystals of $Li_6(NpO_2)_4(H_2Si_2O_7)(HSiO_4)_2(H_2O)_4$ (*LiNpSi1*) and $K_3(NpO_2)_3(Si_2O_7)$ (*KNpSi1*) were prepared by the addition of 0.15 mL of the neptunyl stock solution (162 mM Np^{5+}) and 0.35 mL of 50 mM aqueous silica solution (prepared using silica gel from Sigma-Aldrich, #214418-100g, grade 15, 30−60 mesh, batch #08923JC) to a 7 mL Teflon cup with a screw-top lid. The pH of the solution was

(17) Bessonov, A. A.; Grigor'ev, M. S.; Ioussov, A. B.; Budantseva, N. A.; Fedosseev, A. M. *Radiochem. Acta* **2003**, *91*, 339.
(18) Andreev, G. B.; Fedoseev, A. M.; Perminov, V. P.; Budantseva, N. A. *Radiokhimiya* **2003**, *45*, 488.
(19) Burns, P. C.; Ewing, R. C.; Miller, M. L. *J. Nucl. Mater.* **1997**, *245*, 1.
(20) Burns, P. C.; Deely, K. M.; Skanthakumar, S. *Radiochim. Acta* **2004**, *92*, 151.
(21) Burns, P. C.; Klingensmith, A. L. *Elements* **2006**, *351*, 351.
(22) Klingensmith, A. L.; Deely, K. M.; Kinman, W. S.; Kelly, V.; Burns, P. C. *Am. Mineral.* **2007**, *92*, 662.
(23) Forbes, T. Z.; Burns, P. C.; Soderholm, L.; Skanthakumar, S. *Chem. Mater.* **2006**, *18*, 1643.
(24) Forbes, T. Z.; Burns, P. C. *J. Solid State Chem.* **2007**, *180*, 115.
(25) Albrecht-Schmitt, T.; Almond, P. M.; Sykora, R. *Inorg. Chem.* **2003**, *42*, 3788.
(26) Albrecht-Schmitt, T. E.; Almond, P. M.; Sykora, R. E. *Inorg. Chem.* **2003**, *42*, 3788.
(27) Almond, P. M.; Skanthakumar, S.; Soderholm, L.; Burns, P. C. *Chem. Mater.* **2007**, *19*, 280.
(28) Grigor'ev, M. S.; Baturin, N. A.; Budantseva, N. A.; Fedoseev, A. M. *Radiokhimiya* **1993**, *35*, 29.
(29) Grigor'ev, M. S.; Bessonov, A. A.; Krot, N. N.; Yanovskii, A. I.; Struchkov, Y. T. *Radiokhimiya* **1993**, *35*, 17.
(30) Grigor'ev, M. S.; Yanovskii, A. I.; Fedoseev, A. M.; Budantseva, N. A.; Struchkov, Y. T.; Krot, N. N.; Spitsyn, V. I. *Dokl. Bulg. Akad. Nauk.* **1988**, *300*, 618.
(31) Krot, N. N.; Grigor'ev, M. S. *Russ. Chem. Rev.* **2004**, *73*, 89.
(32) Sullivan, J. C.; Hindman, J. C.; Zielen, A. J. *J. Am. Chem. Soc.* **1961**, *83*, 3373.

Table 2. Bond Lengths (Å) and Angles (deg) for *LiNpSi1*[a]

Np(1)−O(2)	1.84(2)	Si(2)−O(3)	1.50(2)
Np(1)−O(6)	1.85(2)	Si(2)−O(5)	1.54(2)
Np(1)−O(5)[a]	2.38(1)	Si(2)−O(9B)	1.64(3)
Np(1)−O(5)[b]	2.38(1)	Si(2)−O(7)	1.62(3)
Np(1)−O(7)	2.45(2)		
Np(1)−O(3)	2.52(1)	Li(1)−O(10)	1.95(5)
Np(1)−O(3)[c]	2.52(1)	Li(1)−O(9A)[f]	2.09(4)
O(2)−Np(1)−O(6)	179.5(7)	Li(1)−O(9A)[g]	2.09(4)
		Li(1)−O(9B)	2.16(5)
Np(2)−O(1)	1.85(2)	Li(1)−O(9B)[d]	2.16(5)
Np(2)−O(4)	1.85(2)	Li(1)−O(2)[g]	2.28(5)
Np(2)−O(7)[a]	2.44(2)		
Np(2)−O(3)[d]	2.41(1)	Li(2)−O(4)[h]	2.04(8)
Np(2)−O(3)	2.41(1)	Li(2)−O(1)	2.01(7)
Np(2)−O(5)[e]	2.50(1)	Li(2)−O(6)[i]	2.05(8)
Np(2)−O(5)[a]	2.50(1)	Li(2)−O(8)[i]	2.31(2)
O(1)−Np(2)−O(4)	179.5(7)	Li(2)−O(8)[j]	2.31(2)
Si(1)−O(10)	1.65(2)	Li(3)−O(9A)	1.86(6)[k]
Si(1)−O(5)	1.64(2)	Li(3)−O(8)	1.89(6)
Si(1)−O(3)	1.65(2)	Li(3)−O(9B)	2.02(7)[k]
Si(1)−O(9A)	1.67(3)	Li(3)−O(2)	2.14(6)[l]
		Li(3)−O(4)	2.16(6)[l]

[a] Symmetry transformations used to generate equivalent atoms: a: $-x + 1/2, -y, z + 1/2$; b: $-x + 1/2, y - 1/2, z + 1/2$; c: $x, -y - 1/2, z$; d: $x, -y + 1/2, z$; e: $-x + 1/2, y + 1/2, z + 1/2$; f: $-x + 1, y + 1/2, -z + 1$; g: $-x + 1, -y, -z + 1$; h: $x - 1/2, y, -z + 3/2$; i: $-x, -y, -z + 1$; j: $-x, y + 1/2, -z + 1$; k: $x - 1/2, y, -z - 1/2$; and l: $-x + 1/2, -y, z - 1/2$.

adjusted to ~12 using 300 μL of a 1 M LiOH and 3 M KOH solution for *LiNpSi1* and *KNpSi1*, respectively. The initial solutions were bright green, but upon addition of the base, a greenish-gray precipitate formed. The sealed Teflon cups were placed in a 125 mL Teflon-lined Parr acid digestion vessel with 35 mL of 18 MΩ ultrapure water added to provide counterpressure during heating. The samples were heated in a gravity convection oven at 200 °C for 1 week. After the heating cycle, the samples were slowly cooled to room temperature. Dark-green plates of *LiNpSi1* approximately 200 μm in length and similarly sized clusters of *KNpSi1* were obtained.

Structure Determination. A suitable single crystal of each compound was mounted on a tapered glass fiber for collection of X-ray diffraction data. A sphere of data was collected for each compound at room temperature using a Bruker single-crystal X-ray diffractometer equipped with an APEX II CCD detector. The data were collected using monochromatic Mo Kα radiation ($\lambda = 0.71073$ Å) with frame widths of 0.3° in ω and a counting time per frame of 30 and 60 s for *LiNpSi1* and *KNpSi1*, respectively. Unit cell parameters, data integration, and corrections for Lorentzian and polarization parameters were completed using the APEX II suite of software.[33] Semiempirical absorption corrections were applied using the Bruker program XPREP by modeling the crystals of *LiNpSi1* as a (001) plate and *KNpSi1* as an ellipsoid. Selected data collection parameters and crystallographic information are provided in Table 1.

The structures of *LiNpSi1* and *KNpSi1* were solved by direct methods and refined on the basis of F^2 for all unique data using the Bruker SHELXTL version 5.01 software.[34] Atomic scattering factors for each atom were taken from the International Tables for X-ray Crystallography.[35] The Np and K atoms were located in the direct solution, and the Si, O, and Li atoms were located in difference Fourier maps calculated following subsequent least-squares refinement of the partial-structure models. *LiNpSi1* is orthorhombic, space group *Pnma*, while *KNpSi1* crystallizes in the hexagonal space group $P\bar{6}2m$. The Np and K atoms were modeled using anisotropic displacement parameters. Both compounds involved partially occupied Si sites; thus, the presence of silicon in each compound was verified by energy dispersive spectroscopy using a LEO EVO-50XVP variable pressure/high humidity scanning electron microscope. H atoms were not located. The selected interatomic distances are provided in Tables 2 and 3 for *LiNpSi1* and *KNpSi1*, respectively. Additional details of the crystal structure analyses can be found in the Supporting Information.

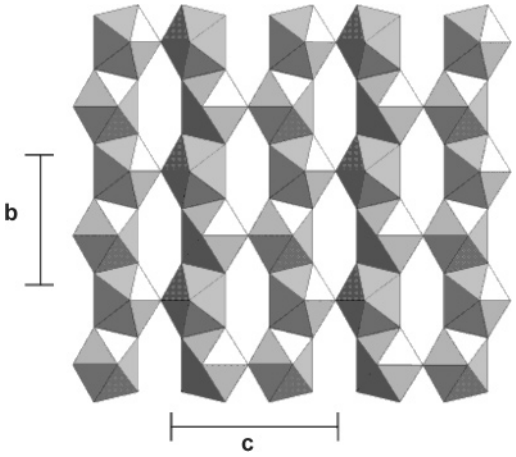

Figure 1. Neptunyl pentagonal bipyramids in *LiNpSi1* share the O(3)−O(5) edge to create chains of neptunyl polyhedra extending in the (010) direction. Adjacent chains share the O(7) vertex to create a two-dimensional sheet of neptunyl polyhedra.

Table 3. Bond Lengths (Å) and Angles (deg) for *KNpSi1*[a]

Np(1)−O(2)	1.785(12)	K(1)−O(1) × 2[h,i]	2.609(7)
Np(1)−O(1)	1.831(11)	K(1)−O(2) × 4[g,j,d]	2.924(5)
Np(1)−O(4) × 4[a,b,c]	2.441(5)	K(1)−O(4) × 2[a,d]	2.947(9)
O(2)−Np(1)−O(1)	180.0(6)		
Si(1)−Si(1)[d]	0.552(12)		
Si(1)−O(4) × 3[e,f]	1.608(7)		
Si(1)−O(3)[g]	1.665(6)		

[a] Symmetry transformations used to generate equivalent atoms: a: y, x, z; b: $y, x, z - 1$; c: $x, y, z - 1$; d: $-x + y, -x, -z + 1$; e: $-x + y, -x + 1, -z + 1$; f: $-y + 1, x - y + 1, z$; g: $x, y, z + 1$; h: $-y + 1, x - y, z$; i: $-y + 1, x - y, z + 1$; and j: $-x + y, -x, -z$.

Results

Structural Description of LiNpSi1. *LiNpSi1* contains two symmetrically independent Np^{5+} atoms that are each strongly bonded to two O atoms, forming a nearly linear dioxo cation. The neptunyl ion bond lengths range from 1.84(2) to 1.85(2) Å. Five equatorial oxygen atoms coordinate the NpO_2^{+} cations to create pentagonal bipyramids that are capped by the neptunyl ion oxygen atoms. The $Np-O_{eq}$ (eq = equatorial) bond lengths range from 2.38(1) to 2.52(2) Å. The structure contains two Si sites located 0.58(1) Å apart, each

Infrared Spectroscopy. The infrared spectra were obtained for single crystals of *LiNpSi1* and *KNpSi1* using a SensIR technology IlluminatIR FT-IR microspectrometer. A single crystal was placed on a glass slide, and the spectrum was collected with a diamond ATR objective. The spectrum was taken from 600 to 4000 cm^{-1} with an aperture of 100 μm.

(33) *APEX Software*; Bruker: Madison, WI, 2005.
(34) *SHELXTL, version 5.01*; Bruker: Madison, WI, 1998.
(35) Ibers, J. A.; Hamilton, W. A. *International Tables for X-ray Crystallography*; Kynoch Press: Birmingham, U.K., 1974; Vol. IV.

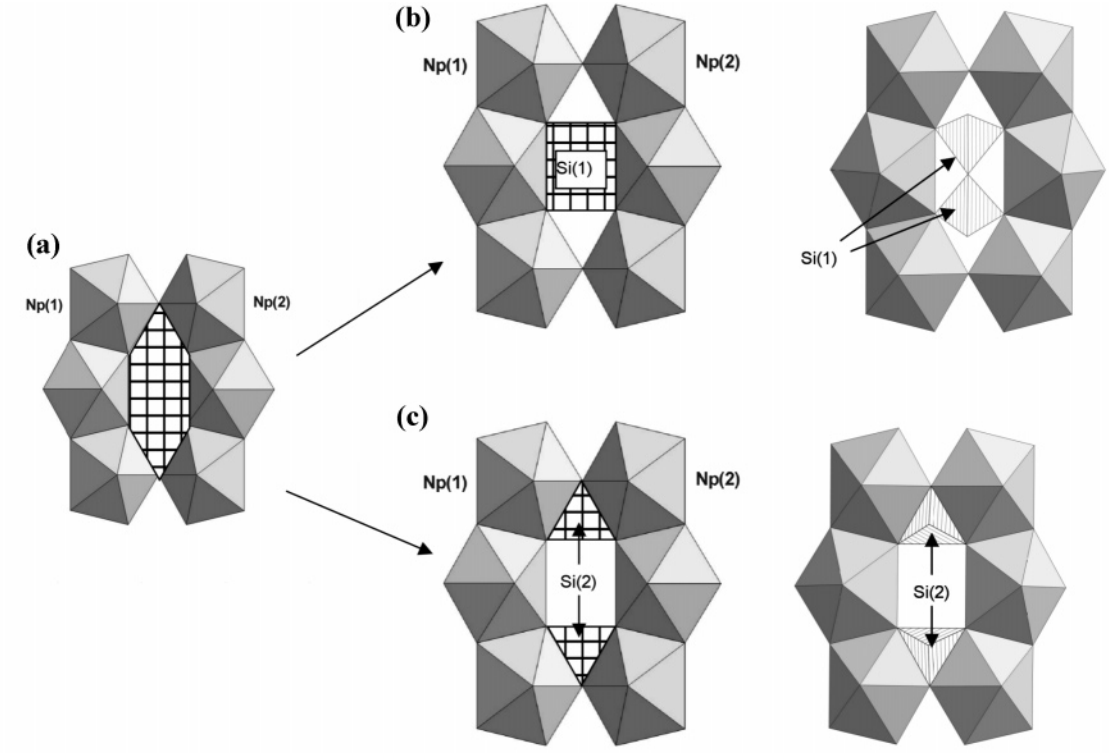

Figure 2. (a) Large hexagonal void spaces are created between the chains of neptunyl pentagonal bipyramids in *LiNpSi1*. Two silicate sites are located within the void spaces. (b) Si(1) site is located in the central square of the void space. Two silicate tetrahedra share an apical O atom to create a sorosilicate dimer. (c) Si(2) site is located in the end triangles. Nesosilicate units share the equatorial edges of adjacent neptunyl pentagonal bipyramids.

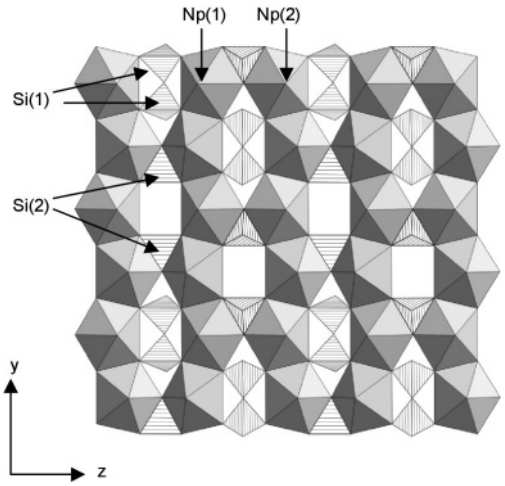

Figure 3. Hexagonal void spaces created by the chains of neptunyl polyhedra in *LiNpSi1* are either occupied by a Si(1) dimer or by two Si(2) monomers, and these configurations alternate along the *b*-direction.

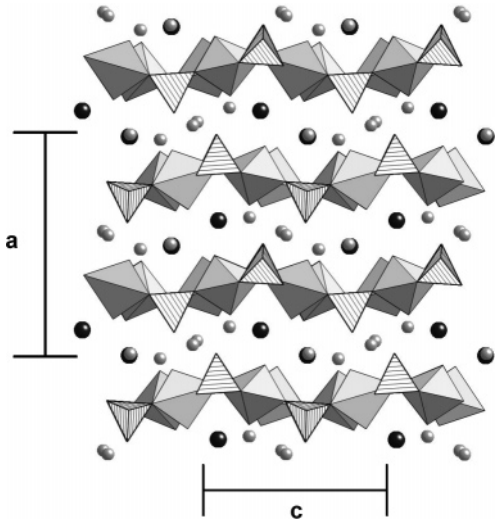

Figure 4. Charge balancing Li^+ cations (black spheres) and H_2O groups (gray spheres) are located between the neptunyl silicate sheets in *LiNpSi1*.

of which is 50% occupied. Anions are impacted by the partial occupancy of the Si sites. The O(7) site is displaced from the mirror plane, such that it is 0.69(5) Å from its symmetry equivalent, and it is 50% occupied. The O(9) atom is equally distributed over two sites (O(9A) and O(9B)) separated by 0.86(4) Å. Finally, the O(10) site is 50% occupied.

The neptunyl pentagonal bipyramids share the equatorial edge defined by O(3) and O(5), resulting in a chain of pentagonal bipyramids one polyhedron wide that extends along the *b*-axis (Figure 1). Adjacent chains of pentagonal bipyramids share the O(7) vertex, which results in a sheet that is parallel to (100). The silicate tetrahedra are associated with the large voids within the sheet, as highlighted in Figure 2. There are two distinctly different configurations. If the Si(1) site is occupied, it is coordinated by the O(3), O(5), O(9A), and O(10) anions, with an average bond length of 1.65 Å. Symmetrically equivalent Si(1) tetrahedra share the O(10) vertex, resulting in a sorosilicate dimer. This dimer is attached to the square voids within the sheet of pentagonal bipyramids, such that four of its vertices are equatorial vertices of the neptunyl bipyramids. Two of the vertices of the dimer are terminal and occupied by OH. Thus, where the Si(1) site is occupied, the structure contains a sorosilicate unit with composition $H_2Si_2O_7$. In 50% of the cases, the Si-

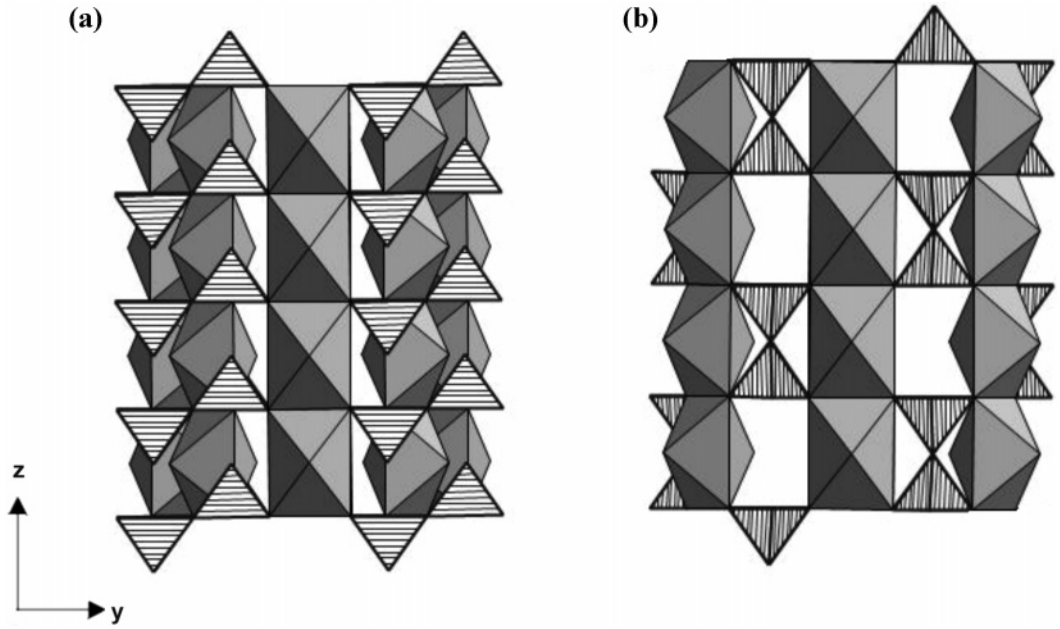

Figure 5. Structure of *KNpSi1* contains chains of neptunyl square bipyramids that are linked together into a framework through sharing of bipyramid vertices with silicate vertices. Because of disorder about the Si(1) atom, two possible structural models exist for *KNpSi1*: (a) isolated silicate tetrahedra with the unshared vertex pointing up in one chain and down in the other and (b) a sorosilicate $(Si_2O_7)^{-6}$ dimer with two silicate tetrahedra sharing one vertex. Infrared spectroscopy confirmed that the sorosilicate model is correct.

(2) site is occupied and is coordinated by the O(3), O(5), O(9B), and O(7) anions, with an average bond length of 1.57 Å. This tetrahedron is located in a triangular void within the sheet of bipyramids, such that three of its vertices, and two of its edges, are shared with the bipyramids. The fourth vertex of the tetrahedron is terminal and is occupied by an OH group. The Si(2) tetrahedron is a nesosilicate unit as it occurs isolated in the structure and has the composition $HSiO_4$.

A plausible local distribution of Si(1) and Si(2) tetrahedra within the sheet of bipyramids is illustrated in Figure 3. Consider the large six-sided voids within the sheet of pentagonal bipyramids (Figure 2a). In this model, these voids are either occupied by a Si(1) dimer (Figure 2b) or by two Si(2) monomers (Figure 2c), and these configurations alternate along the *b*-direction (Figure 3). Note that the Si(2) tetrahedra cannot occur in adjacent six-sided voids along the *b*-direction, as this would cause serious overbonding at the O(7) site. Careful analysis of the diffraction data failed to reveal a doubling of the *b*-unit cell dimension; thus, it is likely that there is disorder of the chain configurations along the *z*-direction and that there is no apparent energetic penalty for such disorder.

Although there is uncertainty in the details of the Li sites because of their low X-ray scattering efficiency, the data indicate three symmetrically independent Li^+ sites in the interlayer. Partial occupancy of some of these sites is required to provide six Li per formula unit. Li(1) is coordinated by six O atoms (five from silicate tetrahedra and one from the Np(1) uranyl ion) with interatomic distances ranging from 1.95(5) to 2.28(5) Å. Five O atoms (three of the neptunyl ions and one interlayer H_2O group) form the coordination sphere around Li(2), with interatomic distances ranging from 2.01(7) to 2.31(2) Å. The Li(3) position is coordinated by five O (two of the neptunyl ions, one interlayer H_2O group, and two from the silicate tetrahedra) atoms with interatomic distances ranging from 1.86(6) to 2.16(5) Å. A H_2O molecule [O(8)] is also located between the neptunyl silicate sheets, where it is coordinated to the Li^+ cations (Figure 4).

Structural Description of KNpSi1. *KNpSi1* contains one symmetrically independent Np^{5+} cation that is strongly bonded to two O atoms, forming a nearly linear NpO_2^+ cation with bond lengths of 1.81(2) and 1.83(2) Å. The neptunyl ion is further coordinated by four oxygen atoms, located at the equatorial vertices of a square bipyramid that is capped by the neptunyl ion oxygen atoms. One crystallographically independent Si site is also located in the structure. The Si(1) atom is displaced from a special position on the 6-fold rotoinversion axis, such that it is 0.55(1) Å from its symmetry equivalent and is 50% occupied. The Si(1) atom is tetrahedrally coordinated with Si−O bond lengths ranging from 1.608(7) to 1.665(6) Å. The apex of the tetrahedron points up in half of the sites and down in the remaining sites.

The neptunyl square bipyramids share the O(4)−O(4) edge, creating chains of neptunyl polyhedra extending in the [001] direction (Figure 5a). The chains of neptunyl polyhedra are linked into an infinite framework through the sharing of vertices with the silicate tetrahedra. Because of the splitting of the Si(1) site, there are two plausible configurations of the tetrahedron. The first consists of isolated silicate tetrahedra with the apex of the tetrahedra pointing up in one chain and down in the neighboring chain (Figure 5a). Three of the O atoms of the silicate tetrahedra are equatorial vertices of neptunyl polyhedra, leaving one unshared O atom. Electroneutrality of the structure is required, and the underbonded state of these unshared O atoms indicate an $(HSiO_4)^{-3}$ group. The second model involves silicate tetrahedra that alternately point up and down within the same chain with a

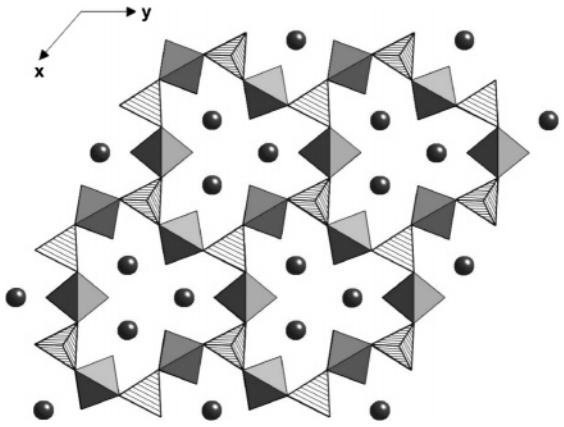

Figure 6. Framework structure of *KNpSi1* contains open channels that are approximately 6.0 Å in diameter and contain charge balancing K^+ cations.

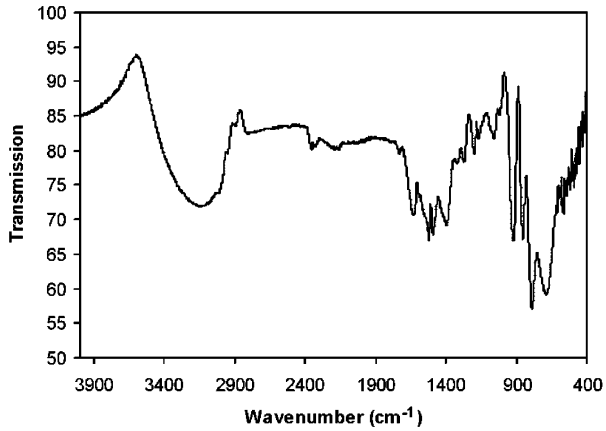

Figure 7. Infrared spectrum of *LiNpSi1*.

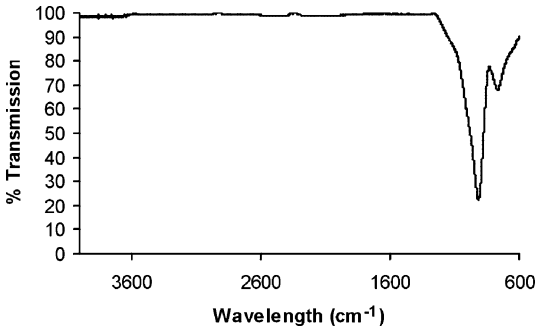

Figure 8. Infrared spectrum of *KNpSi1*.

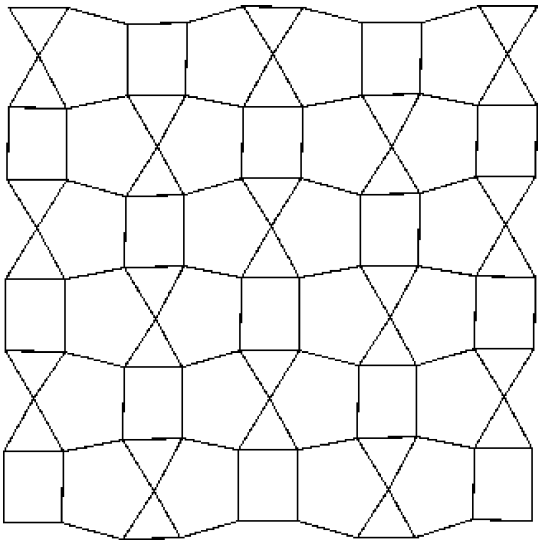

Figure 9. Anion-sheet topology of *LiNpSi1* contains chains of pentagons followed by chains of squares and triangles. This topology is identical to the β-U_3O_8 sheet type, which contains chains of uranyl pentagonal bipyramids and distorted octahedron.

shared vertex between the two silicate tetrahedra (Figure 5b). The resulting coordination creates the $(Si_2O_7)^{-6}$ sorosilicate dimer that then connects the chains of the neptunyl square bipyramid into a three-dimensional framework. The infrared spectrum supports this model with sorosilicate groups and the absence of hydrogen.

The chains of neptunyl square bipyramids and silicate tetrahedra form a framework containing microporous channels (Figure 6). The fundamental building blocks of the channels consist of six chains of neptunyl square bipyramids connected through sorosilicate dimers. Three of the neptunyl polyhedra chains are located on the corners of a triangular channel, and three are at the centers of the faces of three triangles. The neptunyl polyhedra at the centers of the triangular faces are located at the corners of the neighboring triangular channels, creating an interlocked framework of microporous channels.

The pore space of the channels, measured from the apical O atoms on the corner neptunyl polyhedra to the polyhedra at the face center, is approximately 6.0 Å. One crystallographically independent K^+ cation is located in the void space (Figure 6). The K(1) atom is coordinated by eight O atoms with an interatomic distance ranging from 2.62(1) to 2.95(1) Å.

Infrared Spectroscopy. The infrared spectrum of *LiNpSi1* contains two major peaks at 720.7 and 797.1 cm^{-1} that may be assigned to the antisymmetric (ν_{as}) vibrations of the neptunyl moiety (Figure 7). The presence of two neptunyl vibrational modes may be attributed to the two crystallographically distinct Np^{5+} sites in the structure.[31] Peaks at 862.3 and 942.3 cm^{-1} may be assigned to the fundamental vibration modes of the SiO_4 tetrahedra.[36] Generally, the free T_d symmetry of the tetrahedral unit results in four fundamental modes, but only two vibrational modes at 950 cm^{-1} (ν_3) and 530 cm^{-1} (ν_4) are IR active. *LiNpSi1* contains a bridged bidentate silicate complex that lowers the SiO_4 symmetry from T_d to C_{2v} and activates the symmetric stretching vibration (ν_1) at 820 cm^{-1}.[36] A series of smaller peaks located between 1443 and 1564 cm^{-1} can be assigned to the bending vibration of the OH groups at the silicate tetrahedra vertices. This result is in agreement with the crystal structure analysis, which requires acid silicate groups for the overall electroneutrality of the structure. The IR spectrum of *LiNpSi1* also contains free O−H vibrational modes, thus confirming the presence of H_2O in the interlayer between

(36) Cejka, J. Infrared spectroscopy and thermal analysis of the uranyl minerals. In *Uranium: Mineralogy, Geochemistry, and the Environment*; Burns, P. C., Finch, R., Eds.; Mineralogical Society of America: Washington, D.C., 1999; Vol. 38, pp 521−622.

the neptunyl silicate sheets. The diffuse O−H stretching band from 2877 to 3626 cm^{-1} along with a narrow H_2O bending mode at 1661.1 cm^{-1} are consistent with the presence of structural H_2O.[36]

Infrared spectroscopy is very sensitive to H-bonding within solids and can be used to delineate which structural model for *KNpSi1* is correct. Only two peaks are visible in the spectrum: the ν_3 antisymmetric stretch of NpO_2 at 730.0 cm^{-1} and the ν_3 vibrational mode of SiO_4, located at 903.2 cm^{-1} (refs 31 and 36) (Figure 8). The lack of O−H stretching and bending modes discounts the structural model containing isolated acid silicate tetrahedra. The sorosilicate model includes no H, consistent with the spectrum. Thus, the infrared spectrum is consistent with the crystal structure of *KNpSi1* containing neptunyl square bipyramid chains that are linked into a framework by vertex sharing with sorosilicate dimers (Figure 5b).

Discussion

The compounds *LiNpSi1* and *KNpSi1* are the first Np^{5+} neptunyl silicates. Remarkably, both present structural connectivities that depart from those of uranyl silicates. Consider first the sheet structure of *LiNpSi1*. The topological arrangement of the anions within the sheet is easily derived using the approach of Burns et al.[37] and is shown in Figure 9. This is the well-known β-U_3O_8 anion topology that is also the basis for the sheets that occur in the uranyl oxide hydrate minerals ianthinite, $([U_2^{4+}(UO_2)_4O_6(OH)_4(H_2O)_4](H_2O)_5)$,[38] spriggite $(Pb_3(UO_2)_6O_8(OH)](H_2O)_5)$,[39] and wyartite $(CaU^{5+}(UO_2)_2(CO_3)O_4(OH)(H_2O)_7)$.[40] None of these sheets contains silicate, but rather each of the squares in the anion topology are occupied by uranium, giving square bipyramids. β-U_3O_8, ianthinite, and wyartite are each mixed-valence uranium compounds, which perhaps stabilizes this sheet type in the case of uranium.

In the *LiNpSi1* sheet, half of the squares in the sheet anion topology corresponds to the sorosilicate group, such that the four vertices of the silicate tetrahedra shared with the neptunyl pentagonal bipyramids correspond to the vertices of the square. The other silicate tetrahedra occur in the triangles of the anion topology, such that a base of the tetrahedron corresponds to the triangle.

Why do the neptunyl pentagonal bipyramids and silicate tetrahedra in *LiNpSi1* adopt a topology that departs from the known uranyl silicate sheets, despite the same actinide to silicon ratios? The uranophane-type sheet is especially common in uranyl silicates and contains chains of uranyl pentagonal bipyramids that are topologically identical to the chains of neptunyl bipyramids in *LiNpSi1*. However, in the uranophane-type sheet, the chains of bipyramids are not directly linked but rather are connected into a sheet by sharing edges and vertices with silicate tetrahedra. Given that there are no cation−cation interactions in *LiNpSi1*, it seems unlikely that the differences in the strength of the bonds within the neptunyl and uranyl ions result in these different topologies. The neptunyl pentagonal bipyramids are slightly larger than the uranyl analogues, with average equatorial bond lengths of 2.45 Å for the polyhedra in *LiNpSi1*, as compared to an average for uranyl pentagonal bipyramids in well-refined structures of 2.368 Å, with a standard deviation of 0.10 Å.[3] The formal valence is less for Np^{5+} than for U^{6+}. This latter consideration may favor the sharing of edges between silicate tetrahedra and neptunyl bipyramids more so than with uranyl bipyramids. The β-U_3O_8 anion topology that is the basis of the sheet in *LiNpSi1* provides the Si(2) position, for which the tetrahedron shares edges with two bipyramids.

The connectivity of the $H_2Si_2O_7$ sorosilicate group to the sheet of pentagonal bipyramids in *LiNpSi1* warrants further attention. Two vertices of a single edge of a bipyramid correspond to one O atom of both of the silicate tetrahedra in the sorosilicate group. This connectivity has implications for the geometry of the sorosilicate unit. In *LiNpSi1*, the two O atoms of the sorosilicate unit that connect to the same bipyramid are separated by 3.31 Å, and the Si−O−Si bond angle is 137.2°. The length of this edge of the bipyramid is significantly longer than the other four edges, which range from 2.44 to 3.00 Å. The Si−O−Si bond angle is fairly pliable, and the maximum of the distribution of 468 angles in well-refined structures is 139°, which is assumed to be a strain-free Si−O−Si bond angle.[1] Thus, it appears that the sorosilicate unit in *LiNpSi1* is essentially strain-free, but this is achieved by significant distortion of the edge lengths of the neptunyl bipyramid. Even more distortion would be needed to achieve the same connectivity for the uranyl pentagonal bipyramid with its smaller coordination polyhedron, which may explain as to why no uranyl silicates with this connectivity have been observed.

Thirteen neptunyl compounds are known that possess framework structures, but only two of these, *KNpSi1* and $Cs(NpO_2)(MoO_4)(H_2O)$,[41] do not contain cation−cation interactions. The structure of *KNpSi1* bears little resemblance to those of other neptunyl compounds or to the framework uranyl silicates. The large channel within its framework is notable, as only two uranyl structure types have similarly sized channels. The compounds α-$Cs_2[(UO_2)_2(MoO_4)_3]$,[40] $Rb_2[(UO_2)_2(MoO_4)_3]$,[43] and $Tl_2[(UO_2)_2(MoO_4)_3]$[44] contain uranyl pentagonal bipyramids that share all five of their equatorial vertices with molybdate tetrahedra, resulting in a framework with channels in the [001] and [100] directions that are 3.5 × 10.5 and 4.8 × 3.8 Å, respectively. $(NH_4)_2[(UO_2)_5(MoO_4)_7](H_2O)_5$ contains strips of uranyl pentagonal bipyramids and molybdate tetrahedra that spiral about tubular openings with a void space of approximately 7.5 Å in

(37) Burns, P. C.; Miller, M. L.; Ewing, R. C. *Can. Mineral.* **1996**, *34*, 845.
(38) Burns, P. C.; Finch, R.; Hawthorne, F. C.; Miller, M. L.; Ewing, R. C. *J. Nucl. Mater.* **1997**, *249*, 199.
(39) Brugger, J.; Krivovichev, S. V.; Berlepsch, P.; Meisser, N.; Answermet, S.; Armbruster, T. *Am. Mineral.* **2004**, *89*, 339.
(40) Burns, P. C.; Finch, R. *Am. Mineral.* **1999**, *84*, 1456.
(41) Grigor'ev, M. S.; Fedoseev, A. M.; Budantseva, N. A.; Antipin, M. Y. *Radiokhimiya* **2005**, *47*, 545.
(42) Krivovichev, S. V.; Cahill, C. L.; Burns, P. C. *Inorg. Chem.* **2002**, *41*, 34.
(43) Krivovichev, S. V.; Burns, P. C. *J. Solid State Chem.* **2002**, *168*, 245.
(44) Nazarchuk, E. V.; Krivovichev, S. V.; Burns, P. C. *Radiochem.* **2005**, *47*, 447.

diameter.[45] In all of these structures, charge-balancing cations and H_2O groups reside within the channels.

Acknowledgment. This research was supported by the Chemical Sciences, Geosciences and Biosciences Division, Office of Basic Energy Sciences, Office of Science, U.S. Department of Energy, Grant No. DE-FG02-07ER15880.

(45) Krivovichev, S. V.; Cahill, C. L.; Burns, P. C. *Inorg. Chem.* **2003**, *42*, 2459.

Supporting Information Available: Crystallographic CIF files and tables of atomic parameters. This material is available free of charge via the Internet at http://pubs.acs.org.

IC701335J